Geoscientific
Model Development

Open Access

Air quality forecast of PM_{10} in Beijing with Community Multi-scale Air Quality Modeling (CMAQ) system: emission and improvement

Q. Wu[1], W. Xu[2], A. Shi[2], Y. Li[2], X. Zhao[3], Z. Wang[4], J. Li[2], and L. Wang[1]

[1]College of Global Change and Earth System Science, Beijing Normal University, Beijing 100875, China
[2]Beijing Municipal Environmental Protection Monitoring Center, Beijing 100048, China
[3]Environmental Meteorology Forecast Center of Beijing-Tianjin-Hebei, Beijing 100089, China
[4]State Key Laboratory of Atmospheric Boundary Layer Physics and Atmospheric Chemistry (LAPC),
Institute of Atmospheric Physics, Chinese Academy of Sciences, Beijing 100029, China

Correspondence to: Q. Wu (wqizhong@bnu.edu.cn) and X. Zhao (xjzhao@ium.cn)

Abstract. The MM5-SMOKE-CMAQ model system, which was developed by the United States Environmental Protection Agency (US EPA) as the MODELS-3 system, has been used for daily air quality forecasts in the Beijing Municipal Environmental Monitoring Center (Beijing MEMC), as a part of the Ensemble air quality Modeling forecast System for Beijing (EMS-Beijing) since the 2008 Olympic Games. According to the daily forecast results for the entire duration of 2010, the model shows good performance in the PM_{10} forecast on most days but clearly underestimates PM_{10} concentration during some air pollution episodes. A typical air pollution episode from 11–20 January 2010 was chosen, in which the observed air pollution index of particulate matter (PM_{10}-API) reached 180 while the forecast PM_{10}-API was about 100.

In this study, three numerical methods are used for model improvement: first, by enhancing the inner domain with 3 km resolution grids, and expanding the coverage from only Beijing to an area including Beijing and its surrounding cities; second, by adding more regional point source emissions located at Baoding, Landfang and Tangshan, to the south and east of Beijing; third, by updating the area source emissions, including the regional area source emissions in Baoding and Tangshan and the local village/town-level area source emissions in Beijing. The last two methods are combined as the updated emissions method. According to the model sensitivity testing results by the CMAQ model, the updated emissions method and expanded model domain method can both improve the model performance separately. But the expanded model domain method has better ability to capture the peak values of PM_{10} than the updated emissions method due to better reproduction of the pollution transport process in this episode. As a result, the hindcast results ("New(CMAQ)"), which are driven by the updated emissions in the expanded model domain, show a much better model performance in the national standard station-averaged PM_{10}-API. The daily hindcast PM_{10}-API reaches 180 and is much closer to the observed value, and has a high correlation coefficient of 0.93. The correlation coefficient of the PM_{10}-API in all Beijing MEMC stations between the hindcast and observation is 0.82, clearly higher than the forecast 0.54. The FAC2 increases from 56 % in the forecast to 84 % in the hindcast, and the NMSE decreases from 0.886 to 0.196. The hindcast also has better model performance in PM_{10} hourly concentrations during the typical air pollution episode. The updated emissions method accompanied by a suitable domain in this study improved the model performance for the Beijing area significantly.

1 Introduction

In the last 10 years, air quality problems have caused particular concern in most of China, especially after the extreme air pollution episode that happened in multiple cities of North China in January 2013. In such a heavily air-polluted environment, people want access to reasonable air quality predictions, so as to have advance notice of future air pollution events with potential adverse health effects, and so that the government can take necessary short-term emissions reduction measures to improve air quality, as was done during the Beijing Olympic Games. Wu et al. (2010a) and Wang et al. (2010) reported that PM$_{10}$-related emissions were reduced by about 200 tonnes a day at that time. Air quality models are effective tools for air quality forecasts and also to inform policy decisions, since they can provide scientific advice on air pollution control measures (Feng et al., 2007).

The Ensemble Air Quality Modeling Forecast System for Beijing (EMS-Beijing) has been used for air quality forecasting since the 2008 Olympic Games (Wang et al., 2009; Wu, 2010). The ensemble system contains the Community Multiscale Air Quality (CMAQ) modelling system v4.4 (Byun and Ching, 1999; Byun and Schere, 2006), the 3-D Comprehensive Air Quality Model with extensions (CAMx) v4.0 (ENVIRON, 2002) and the Nested Air Quality Prediction Modeling System (NAQPMS) (Wang et al., 2006), using the unified meteorological field and emissions provided respectively by the fifth-generation Mesoscale Model (MM5) and the Sparse Matrix Operator Kernel Emissions (SMOKE) (Houyoux and Vukovich, 1999). All the models adopt the same model domain with the same grid size and resolution, and the system is a good platform for air quality modelling study, to evaluate and improve the models.

The ensemble forecast system has provided successful forecasts since the 2008 Olympic Games, and has been introduced in Shanghai, Guangzhou and other cites (Wu, 2010; Wu et al., 2010a, 2012) in the past few years. In this study, we collect the daily forecast results of the CMAQ model, one member of the EMS-Beijing, for the entire duration of 2010 for the model evaluation. The model shows a good performance on most days but clearly underestimates some air pollution episodes. A typical air pollution episode from 11–20 January 2010 was chosen for the model evaluation and improvement, in which the air pollution index (API) of particulate matter (PM$_{10}$) observed by Beijing MEMC reaches 180 while the CMAQ prediction of PM$_{10}$-API is about 100. Some numerical methods are used for model improvement of the hindcast simulation in this study, involving change of model set-up and updating of emissions.

The remainder of the paper is organized as follows. Section 2 gives the model description and set-up in the forecast system, including meteorological field and air quality model descriptions in Sects. 2.1 and 2.2, the model domain in Sect. 2.3 and the emission inventory and processes of the SMOKE model in Sect. 2.4 – including area, point and mobile source emissions. Section 3 presents the model performance and improvement of the CMAQ model system, the observation data are described in Sect. 3.1 and the model performance in the forecast is detailed in Sect. 3.2. The model improvement methods are presented in Sect. 3.3 – one is enhancement of the inner domain, the other is updating of the anthropogenic emissions, including area and point source emissions. Further details and model evaluation of the improvement are discussed in Sect. 3.3, and Sect. 3.4 presents the model evaluation and discussion of PM$_{10}$ in the model sensitivity testings when the model domain is expanded, when the emissions are updated, and in the hindcast simulation (including all the improvement methods). The conclusions are given in Sect. 4.

2 Model description of the forecast system

The MM5-SMOKE-CMAQ model system, as one model member of the EMS-Beijing, has been used for daily air quality forecasting since 2008. The framework of the model system is shown in Fig. 1: the MM5 model is used to generate the meteorological field, the SMOKE model is applied to deal with the emissions inventory and provides 3-D gridded emission data for the air quality model, and the CMAQ model provides the concentration of the gas- and particle-species for daily air quality forecasts.

2.1 Meteorological field

In the model system, the fifth-generation NCAR/Penn State Mesoscale Model (MM5) v3.6 (Grell et al., 1994) is used to generate the meteorological field for the SMOKE and CMAQ model. The selected schemes for the present study include the simple ice for explicit moisture scheme, the Grell cumulus scheme, the MRF for PBL scheme and the cloud scheme for atmospheric radiation according to the studies of Gao et al. (2007) and Wu et al. (2010b).

As shown in the "Meteorology" segment of Fig. 1, there are five modules to be used: TERRAIN, pregrid, regridder, INTERPF, and MM5. Both the "pregrid" and "regridder" modules are a part of REGRID, which creates the first-guess meteorological field on MM5 grids; the "pregrid" reads the GRIB1-formatted global data and prepares them in MM5 format. In the forecast system, the National Centers for Environmental Prediction (NCEP) Global Forecast System (GFS) data set, taken from ftp://ncep.noaa.gov, with $0.5° \times 0.5°$ spatial resolution, is used as the initial and boundary conditions for the regional meteorological model MM5, and the daily data sets of the 00, 24, 48, 72, 96 h forecast at 20:00 LT on the last day have been downloaded from websites with the wget tool and cron service in Linux. Once the downloading is finished, the cnvgrib tool, which is built from http://www.nco.ncep.noaa.gov/pmb/codes/GRIB2/ to achieve data format conversion between GRIB1 and GRIB2, is used to
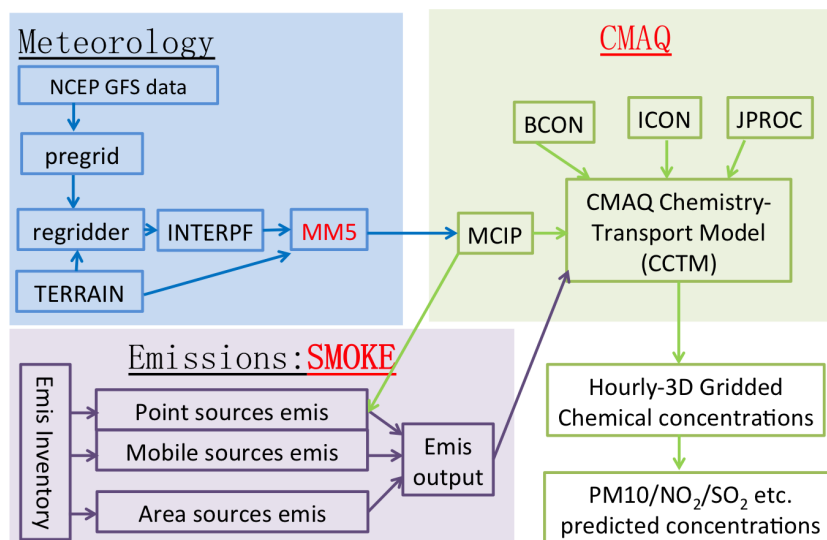
Figure 1. The framework of the MM5-SMOKE-CMAQ forecast system in Beijing.

convert the GRIB2-formatted GFS data sets to GRIB1 format before the "pregrid" module. Then, the MM5 modules begin running to prepare the meteorological field for the emission and air quality model.

For the forecast system, we design csh scripts to schedule the process of the modules, whose scripting feature is to check whether the downloading or the running of the previous module is finished.

2.2 Air quality model descriptions

The CMAQ model is used for regional- and urban-scale air quality simulation of tropospheric ozone, acid deposition, visibility and particulate matter (Byun and Ching, 1999; Byun and Schere, 2006) and has been widely used around the world including in East Asia (An et al., 2007; Zhang et al., 2006). It contains state-of-science parametrizations of atmospheric processes affecting transport, transformation and wet/dry deposition. There are five modules of the CMAQ version 4.4 used in the forecast system as shown in the "CMAQ" segment of Fig. 1. The CMAQ Chemistry-Transport Model (CCTM) is the main module, and the CB-VI scheme for the gas-phase chemistry (Gery et al., 1989), MEBI scheme for the gas-phase chemical solver, RADM scheme for the aqueous-phase chemistry and AERO3 module for aerosol calculation (Binkowski and Roselle, 2003) are applied in the forecast system. The Meteorology Chemistry Interface Processor (MCIP) links MM5 model results with the CCTM module to provide a complete set of the meteorological data needed for the air quality simulations (Appel et al., 2010). The photolysis rate model (JPROC) is used to calculate a day-specific clear-sky photolysis rate look-up table for latitudinal and elevation bands for each photochemical reaction

in the gas-phase chemistry scheme based on work published by Demerjian et al. (1980) (Cruickshank, 2008).

The initial conditions (ICON) and boundary conditions (BCON) are based on clean-troposphere vertical profile concentration fields for the beginning of the first-day simulation and the grids surrounding the outer domain "D1". The initial conditions of the following day simulation are based on the 24 h prediction in the forecast results of the day before. The boundary conditions of the inner domains are retrieved from their mother domain because the CMAQ model uses a one-way nesting scheme in the forecast system – its domain set-up is described in Sect. 2.3.

In this study, we collect the air pollution index (API) as the observation for the model evaluation, which is published on the website of the Beijing Environmental Protection Bureau (Beijing EPB), but only use the primary air pollutant in each station. Particulate material is the primary air pollutant in most cities in North China, such as Beijing, so that PM$_{10}$ has the most observation samples for the model evaluation. The PM$_{10}$ comes from a great variety of emissions sources, including fugitive dust, power plants, cement and pottery manufacturing, while some is produced by oxidization of gaseous pollutant or photochemical reactions as second aerosol – thus, several species must be included in PM$_{10}$ numerical simulation. According to Byun and Ching (1999) and Binkowski and Roselle (2003), the accumulation and Aitken mode of sulfate mass (ASO$_4$), ammonium mass (ANH$_4$), nitrate mass (ANO$_3$), anthropogenic secondary/primary/biogenic organic mass (AORGA/AORGPA/AORGB), elemental carbon mass (AEC), unspecified anthropogenic mass (A25) and coarse mode marine/soil-derived/unspecified anthropogenic mass (ACORS/ASEAS/ASOIL) are included in PM$_{10}$ numerical simulation of the CMAQ model:

$$PM_{10} = ASO_4 + ANH_4 + ANO_3 + AORGA$$
$$+ AORGPA + AORGB + AEC + A25$$
$$+ ACORS + ASEAS + ASOIL. \tag{1}$$

The equation for translation of the concentration to the API is shown in Appendix A. In this study, we translate PM_{10} concentration to PM_{10}-API in the CMAQ model result, to compare with the observed PM_{10}-API in Beijing MEMC stations.

2.3 Model domain

Four nested grids of the horizontal spatial resolution at 81, 27, 9 and 3 km are used for both MM5 and CMAQ models in the forecast system, and the inner two domains (D3 and D4) are shown in the left of Fig. 2.

The centre of the model domain is located at (35.0° N, 110° E) and its two true latitude lines are (30° N, 60° N). The outermost domain (D1) has a 83×65 grid and covers East Asia, while the second domain (D2) has a 61×58 grid to cover North China, which includes the surrounding provinces of the Beijing Municipality – the power plant emissions in those provinces are collected from the Chinese Research Academy of Environmental Sciences (CRAES) as one part of the local emission inventories. The third domain (D3) has 79×70 grids of 9 km resolution and consists of Beijing, Tianjin, most of Heibei province and a part of other surrounding provinces in North China. In Hebei province, as well as the local power plant emission inventory, local inventories of other industrial emissions are collected from Beijing University of Technology (BUT), and handled as point sources. In the forecast system, the fourth domain (D4) has a 73×64 grid and only covers Beijing Municipality, for which more detailed local emissions inventories are included (see Sect. 2.4).

Further, there are 23 sigma vertical layers unequally distributed in the MM5 model with the top layers at 10 hPa and six layers below 1 km; the CMAQ model has 14 vertical layers of which the lower 10 layers are the same as in the MM5 model. The height of the surface (lowest) layer is approximately 35 m.

2.4 Emission inventory and processes

The SMOKE v2.1 (Houyoux and Vukovich, 1999) model is applied to improve the emissions process and provides model-ready emissions for the air quality model. We consider the emissions as area, point and mobile sources in the model system as shown in Fig. 1.

Three emission inventories are used in this study: (1) regional emissions in East Asia from the Transport and Chemical Evolution over the Pacific (TRACE-P) project (Streets et al., 2003; Streets et al., 2006) without the power plant emissions, (2) the Intercontinental Chemical Transport Experiment-Phase B (INTEX-B) power plant emissions inventory with 30 min spatial resolution (Zhang et al., 2009), and (3) local emissions inventories covering the North China region, especially Beijing; emissions inventories were used in Wu et al. (2010c, 2011). The 6 min spatial resolution TRACE-P emissions are handled as area sources while the large point sources (lps sector in TRACE-P emission) are treated as point sources. The INTEX-B power plant emissions are taken as point source emissions and replace the power plant emissions in TRACE-P emissions, and the local emission inventories are taken as area, point and mobile source emissions, as detailed in the following section.

2.4.1 Area source emissions

The area source emissions are taken with a "top-down" approach – the given total emissions are assigned to model grid boxes with a relative spatial distribution factor, such as population or road density. As shown in Fig. 3, the area emissions were spatially allocated according to the Land Scan 2005 Global Population Database (Dobson et al., 2000) and other spatial distribution factor, such as road density; the emissions temporal variation is assigned from a "profile" file, while the species allocation is based on the SPECIATE 4.0 species database (Mobley et al., 2007).

Usually, the statistics emission inventories in China are at the county level, or city level, or even provincial level, from statistics in the administrative boundaries. In order to facilitate updating of the local emission inventories, we transform all regional area source emission inventories into county-level inventories. In the forecast system, the TRACE-P industry (ind), transportation (tra), domestic biofuel (dob), domestic fossil fuel (dof) emissions, livestock ammonium emissions and biogenic emissions (Streets et al., 2003) are converted from latitude–longitude gridded to county-level emission inventories using the geographical statistics tool in ArcGIS platform.

The local area source emissions inventories in Beijing include residential fossil fuel (dof), residential biofuel (dob), unorganized industrial area source, building operations and mutation fugitive dust emission, road fugitive dust emission and anthropogenic ammonia emission; they are county-level inventories in the forecast system. In the SMOKE model system, the residential fossil fuel (dof) and residential biofuel (dob) emissions are used to replace the domestic fossil fuel (dof) and domestic biofuel of the TRACE-P emission in Beijing counties. The other categories of emissions are added directly. In order to obtain high-resolution emissions, the residential area source emissions in Beijing are allocated based on the Land Scan population data – the spatial distribution of the population in Beijing Municipality is shown in the right-hand panel of Fig. 3. Also, the road fugitive dust emission essentially from road surface is spatially distributed according to traffic density in Beijing, with the compiled road statistics including arterial and local roads.
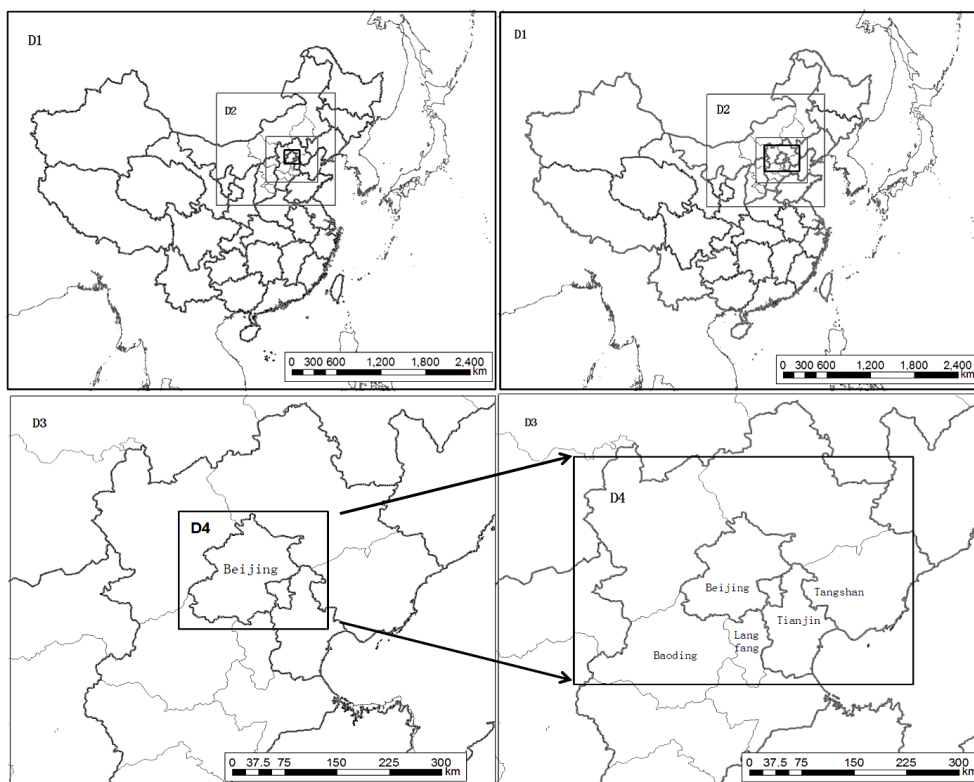
Figure 2. The four-nest domain used in the forecast system and the "new" enhanced domain in the hindcast. Left, the forecast system: D1 covers East Asia with 81 km horizontal resolution and 83×65 grids. D2 includes North China as shown in the upper panel. D3 consists of Beijing, Tianjin and most of Heibei province, but D4 only covers Beijing Municipality with 73×64 grids of 3 km resolution as shown in the lower left panel. On the right, the domain for the "new" simulation (hindcast) in this study – we enlarge the inner D4 domain with 160×124 grids of 3 km resolution, to cover Beijing and its surrounding municipal cities, including Tianjin, Baoding, Langfang and Tangshan.

The spatial distribution of area source emissions in the inner domain (D4) of the forecast system is presented in Fig. 3 – it can be seen that the high-PM$_{10}$ emissions correspond to high-population density, with the highest emission being located in urban Beijing.

2.4.2 Point source emissions

Point source emissions processing in the SMOKE model focuses on converting annual, daily or hourly emissions to hourly, gridded model-ready emissions to be used by the air quality model (UNC, 2010). As with the area source emissions, the temporal variation and species allocation of point source emissions are given by a "profile" file.

The spatial allocation of point source emissions in SMOKE is very straightforward – the procedure simply determines which cell the point source's longitude–latitude coordinates are in and assigns them to model grid cells. Based on the Briggs algorithm (Briggs, 1972, 1984), the SMOKE model uses the stack and meteorological parameters to compute the plumes' distributions into the vertical layers that the plumes intersect, and puts the emissions into the vertical layers. The stack parameters, including the stack height,

diameter and exit gas temperature, are collected from the point source emission inventory; the meteorological parameters are retrieved from the MM5 model results with the MCIP module (Houyoux et al., 1999).

As mentioned above, the point source emissions used in the forecast system include the TRACE-P large point source (lps), $0.5°$ INTEX-B power plant emissions and the local point source emissions. The power plant emissions of the local database cover Beijing and its surrounding provinces including Tianjin, Hebei, Shanxi, Inner Mongolia and Shandong provinces, with the base year of 2006. The local emission inventories have more specific information about the position, and are used to replace the INTEX-B power plant emissions in those provinces. But between 2006 and 2008, some introduction of cleaner combustion and flue gas treatment in power plants has taken place, step by step, including dust control improvement, closure of high-pollution small units, addition of desulfurization patenting agent and low-NO$_x$ combustion. Thus, the power plant emissions in Beijing have been updated according to Hao et al. (2008) and the National "The Coal-Fuel Units Flue Gas Desulfurization Construction Notice" (http://www.sepa.gov.cn/info/gw/gg/200703/t20070308_101419.htm).
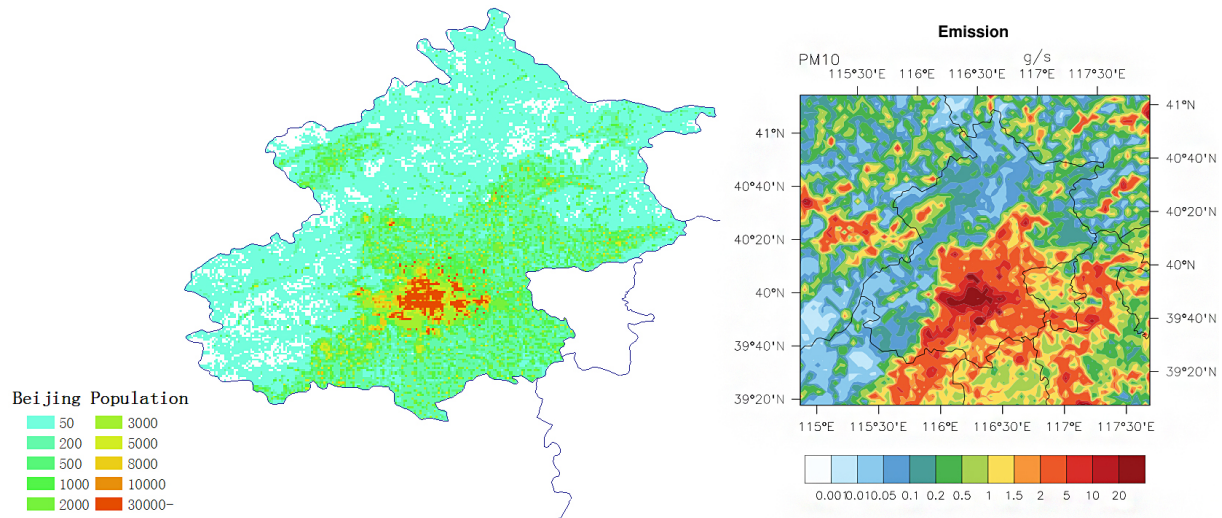
Figure 3. The SMOKE area emissions are spatially allocated based on a related spatial factor, such as population data from the Land Scan 2005 Global Population Database (Dobson et al., 2000). The left panel shows the spatial distribution of the population in Beijing Municipality in the Land Scan 2005; the right panel shows the spatial distribution of PM$_{10}$ emissions in the inner domain in the forecast system.

In Hebei province, there are 418 point source emissions collected and introduced into the point source inventory of the SMOKE model – including the main industrial emissions in Hebei province from Beijing University of Technology (BUT) – which is used by Wu et al. (2011). In Tianjin and Beijing Municipality, there are more detailed point source emissions with full stack parameters, which are provided by CRAES and Beijing Municipal Environmental Protection Bureau (Beijing EPB), and used to update the heating boiler, steel, cement and other industrial emissions in Tianjin and Beijing. In that emissions inventory, there are 493 higher point source emissions, with stack height above 45 m, 1970 lower point source emissions in Tianjin, and 652 point source emissions in Beijing. These local point source emissions are used to replace the related category emissions in the SMOKE model.

2.4.3 Mobile source emission

Based on the road network and the traffic flow data from Beijing Transport Research Center (BTRC, 2007), Wu et al. (2010c) estimated the spatial distribution of the mobile source emissions using the SMOKE mobile module, and used this to assess the impact of vehicle traffic restriction on air quality in Beijing from 17 to 20 August 2007.

The on-road mobile source emissions without vehicle traffic restriction in that study (Wu et al., 2010c) have been used in the EMS-Beijing forecast system, the criteria emission factors using MOBILE6 are computed with the forecast meteorology data (UNC, 2010), and the meteorological field is provided from the everyday MM5 model results through the MCIP module. The mobile source emissions provide 90 % of CO, 50 % of NO$_x$ and 45 % of VOC emissions, but only

a small percentage of SO$_2$, PM$_{10}$ and PM$_{2.5}$ emissions in Beijing in the forecast system.

2.4.4 The total emission

The total emissions used in the forecast system are calculated from the daily report of the SMOKE model output, as shown in Table 1 with other published inventories. Comparing those emission inventories, we found that there is much uncertainty in the emission inventory. For example, in Beijing the CO emission range is from 1021.8 kt yr^{-1} in An et al. (2007) to 2591.0 kt yr^{-1} in Zhang et al. (2009), and the PM$_{10}$ emission ranges from about 66.0 in Streets et al. (2007) to 168.0 kt yr^{-1} in Zhao et al. (2012). The PM$_{2.5}$ emission has the biggest uncertainty, with only 27.2 kt yr^{-1} estimated by Streets et al. (2007), and 162.0 kt yr^{-1} by Cao et al. (2011). The uncertainty comes from the emissions data, the base year of the investigation, the emission factor of each sector, the active rates (e.g. energy consumption or industrial production), and other sources.

The forecast system has the lowest NO$_x$ and VOC emissions in Beijing compared with those studies. The NO$_x$ and VOC emissions, of which the mobile source emissions contributed nearly a half, may be underestimated in the forecast system. The mobile source emissions in Beijing have been estimated based on the investigation of road networks and traffic flow data in 2006 that underestimates the vehicle numbers and traffic flow, and therefore underestimates the CO, NO$_x$ and VOC emissions.

The forecast system also has the lowest emissions of SO$_2$ in Beijing because it includes "Flue Gas Desulfurization" to decrease SO$_2$ emissions in the inventory. In the annual report "State of the Environment Bulletin" published by Beijing

Table 1. Emission of major anthropogenic species (unit: 10^3 t yr^{-1}).

Species	Region	CO	NO_x	VOCs	NH_3	SO_2	PM_{10}	$PM_{2.5}$
In forecast system	Beijing	1793.8	200.0	244.2	121.8	78.8	162.1	59.1
	Tianjin	1609.9	275.3	270.7	47.2	353.5	194.1	132.7
	Hebei	6504.3	983.1	839.6	837.0	1966.7	997.6	712.4
An et al. (2007)	Beijing	1021.8	227.3	285.6	69.1	211.3	106.9	53.4
	Tianjin	737.0	178.9	270.0	50.0	375.9	93.5	38.0
	Hebei	6806.0	686.0	855.0	846.5	1353.7	535.1	264.1
Streets et al. (2007)*	Beijing	2340.0	212.4	339.6	150.0	318.0	66.0	27.2
	Tianjin	1704.0	272.4	272.4	118.9	409.2	80.5	31.6
	Hebei	6540.0	704.4	864.0	1812.0	1272.0	463.2	199.2
Zhang et al. (2009)	Beijing	2591.0	327.0	497.0	–	248.0	123.0	90.0
	Tianjin	1860.0	365.0	381.0	–	336.0	161.0	109.0
	Hebei	15 505.0	1308.0	1521.0	–	2281.0	1371.0	981.0
Cao et al. (2011)	Beijing	1998.0	437.0	744.0	117.0	172.0	–	162.0
	Tianjin	1625.0	337.0	467.0	102.0	263.0	–	151.0
	Hebei	12 669.0	1634.0	2327.0	994.0	2318.0	–	1172.0
Zhao et al. (2012)	Beijing	2580.0	309.0	346.0	87.0	187.0	168.0	90.0
	Tianjing	1326.0	177.0	224.0	74.0	259.0	186.0	100.0
	Hebei	12 202.0	1092.0	757.0	1031.0	1622.0	2291.0	1214.0

* Streets et al. (2007): for July 2001, convert unit Gg mol^{-1} to Gg yr^{-1}.

EPB, the SO_2 emission in the year 2010 was 10.4×10^4 tons (Beijing EPB, 2011). Thus, the SO_2 emission in the forecast system for the year 2010 in Beijing is reasonable but may be underestimated.

3 Model performance and improvement

In this study, we collect the observation and forecast results for the entire duration of 2010 for the model evaluation and improvement. One typical air pollution episode, for which the forecast cannot give the expected peak, is chosen and studied in this section.

3.1 Observation data for model evaluation

There are 27 stations in the Beijing Municipal Environmental Monitoring Center (Beijing MEMC) air quality monitoring network in the year 2010 with the locations shown in Fig. 5. Twelve are the National Standard Air Quality Observation Stations (NSAQ Stations) which are marked as "squares" in Fig. 5 – eight stations are in urban Beijing, three stations are in county towns, and Dingling is the regional background NSAQ station. Except for Dingling, the other 11 stations are located in urban areas, which include cities, towns or conurbations. The air pollution index (API) value is reported daily and published at the website http://www.bjepb.gov.cn/bjepb/341240/index.html. The averaged PM_{10}-API in the NSAQ stations have been collected as observations for the model evaluation, and the daily reported

APIs of the main pollutant in all 27 stations have been also collected as observations and compared with CMAQ model outputs.

The PM_{10} hourly concentration averages at NSAQ stations are provided by Beijing MEMC and used for the evaluation of the model's ability to reproduce the hourly concentration. The PM_{10} hourly concentration of Beijing's surrounding areas are also collected to evaluate the model performance in the surrounding areas (presented in the Supplement). The paper focuses on the model performance in Beijing.

3.2 Model performance in the forecast

In this study, the daily forecast results of the CMAQ model for the entire duration of 2010 are collected for the model evaluation. The scatter diagram of the averaged PM_{10}-API in the NSAQ stations and the forecast are shown in Fig. 6. As shown in the figure, most observed and forecast points are close to the model perfect line "$y = x$", which indicates that the model in the forecast shows a good performance on most days. However, all of the observed–forecast points are below the line "$y = 150$" through some points can reach the line "$x = 250$". This illustrates that the forecast PM_{10}-API is lower than 150 but that observations can reach 250. The forecast results are underestimated when the PM_{10}-API value is high, which is when a serious air pollution episode occurred.

As mentioned above, the model in the forecast shows a good performance on most days but clearly underestimates some air pollution episodes. In order to improve the model
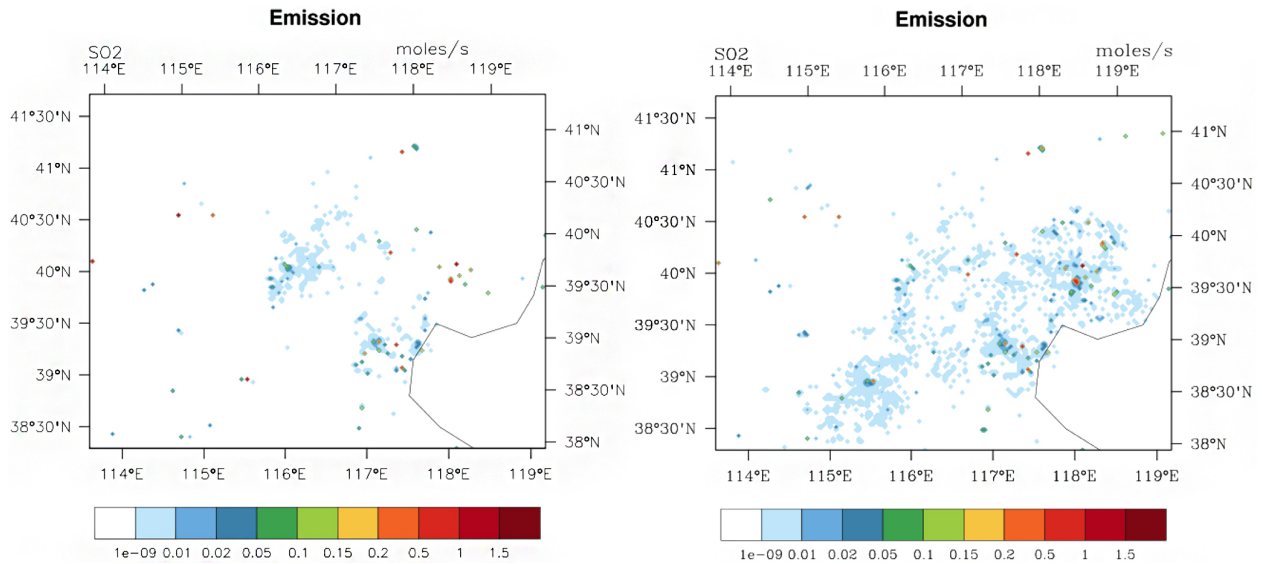
Figure 4. The point source emissions in the "new" D4 domain. Left: the point source emissions in the forecast system; right: the "new" simulation – more point source emissions in Tangshan, Baoding and Langfang have been added.
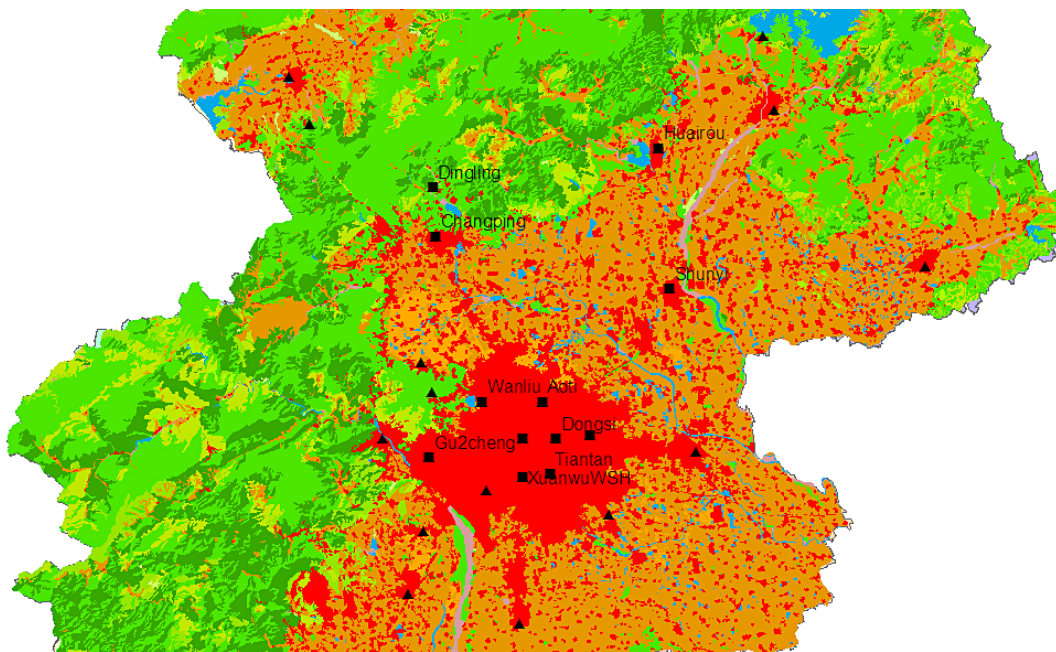

Figure 5. Map of the stations of Beijing MEMC air quality monitoring network. Black shows the location of each observation station – squares are the National Standard Air Quality Observation Stations (NSAQ Stations) and triangles are the other air quality observation stations in the monitoring network. The shading indicates land use: red shading indicates urban area, dark green indicates forest, light green indicates grass, orange indicates crop, blue indicates water.

performance, a typical air pollution episode from 11–21 January 2010 was chosen, in which the averaged air pollution index of particulate matter (PM$_{10}$-API) in NSAQ stations in Beijing reaches 180, while the CMAQ prediction is about 100 as shown in Fig. 7. The green solid line in Fig. 7 presents the averaged PM$_{10}$-API prediction in the 10 NSAQ stations

in Beijing, which is predicted by the CMAQ model in the forecast system, and compared with the observed "red solid line" to show its model performance. It can be seen that the CMAQ model underestimates the peak value during the air pollution episode of 19 January.
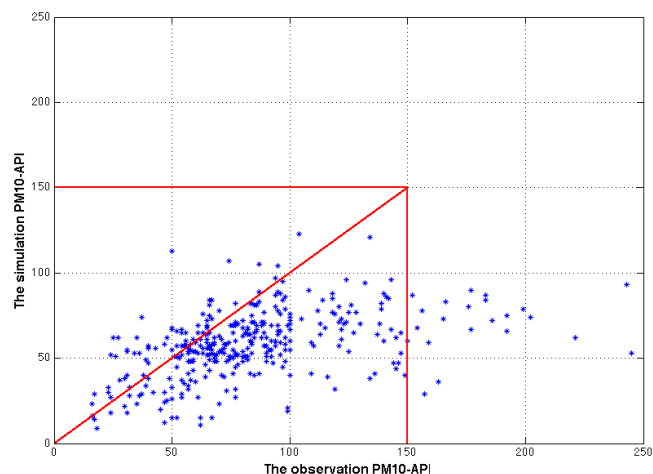
Figure 6. The observed–simulated scatter diagram of the averaged PM$_{10}$-API in the Beijing NSAQ stations in 2010. The averaged NSAQ stations include Aoti, Dongsi, Wanliu, Chegongzhuang, Gu2cheng, Tiantan, XuanwuWSH, Nongzhanguan, Changping, Shunyi and Huairou stations.

As well as the averaged PM$_{10}$-API in NSAQ stations, the main pollutant APIs in all 27 stations – not only NSAQ stations but also non-NSAQ stations, marked as triangles in Fig. 5 – were also collected to verify the modelled PM$_{10}$. The main pollutant in all 27 stations during the typical episode was almost always PM$_{10}$. There were 270 API samples collected – 199 of those samples are marked as "PM$_{10}$, which is the main pollutant", six samples are SO$_2$, and the other samples are "degree I" (that are not marked as the main pollutant). Thus, more than 97 % of the main pollutant in Beijing is PM$_{10}$. In fact, the main pollutant in "degree I" samples is also PM$_{10}$, as confirmed by Beijing MEMC. The missing PM$_{10}$ samples in these 27 stations are also completed by Beijing MEMC.

Compared with the observations, the maximum of the PM$_{10}$-API in all stations predicted by the CMAQ model in the forecast did not exceed 150 during the air pollution episode, but the observed maximum reached 300, as shown in the "red" scatter diagram of Fig. 8.

3.3 Model improvement

In this study, three numerical methods were used for the improvement of air quality forecasting in Beijing.

First, we enlarged the inner domain, the D4 domain with 3 km resolution grids, from which the forecast results are obtained. The original domain in the forecast system only covers Beijing Municipality, with 73 × 64 grids of 3 km resolution. In the new simulation, the western boundary of the domain is moved westward to the western boundary of Hebei province, the northern to the northern boundary of Hebei province, the eastern to the eastern boundary of Hebei province, and the southern to Tianjin Municipality. As shown

in Fig. 2, the new D4 domain has 160 × 124 grids, and covers Beijing and its surrounding cities, including Zhangjiakou, Chengde, Tangshan, Langfang, Baoding and Tianjin Municipality.

Second, we added more point source emissions into the SMOKE model, especially in the cities to the south and east of Beijing, to improve the model performance. To the south, 1935 point sources in Baoding have been added into the point source emissions inventory of the SMOKE model. Baoding plays an important role in the PM$_{10}$ contribution in the urban area of Beijing and its southern counties (Wu et al., 2011). Landfang is another municipality that contributes a lot of PM$_{10}$ concentration to Beijing – it is to the southeast of Beijing and has a dominant role in the surrounding area contribution to Beijing's eastern counties (Wu et al., 2011). Therefore, the point source emissions in Landfang are also collected to improve the simulation, and there are 609 point source emissions that have been added. Tangshan is to the east of Beijing, and is the biggest emissions municipality in Hebei for SO$_2$, NO$_x$ and particle matter emissions (CC-CPSC, 2011) – 1861 point source emissions in Tangshan have been added. These additional 4405 point source emissions include industrial, commercial and other categories. Their locations have been checked with Google Earth and other tools, to improve the accuracy of the emission intensity and location data in Baoding, Landfang and Tanshan. The distribution of the point source emissions in the "new" D4 domain is shown in the right panel of Fig. 4.

Third, the area emissions were updated. The area emissions in Baoding and Tangshan, which are the two key cities for air pollutants, were increased according to the emissions report in CCCPSC (2011), and the total emissions of Baoding and Tangshan are shown in that emissions report. In order to get more accurate emissions, the Beijing stationary area emission inventory is updated from the statistical county level to the village–town level, to provide more detailed spatial information for area emissions in Beijing. There are 18 counties in the forecast system, and more than 100 village–towns in the new simulation, so the statistical unit of area emissions has been greatly refined, bringing more accuracy to the distribution of the emissions.

3.4 Model performance in the new simulation

The improvement methods mentioned above comprise two aspects: one is the enhancement of the inner domain, and the other is the updating of the emissions, including area and point source emissions. The model sensitivity testings of the CMAQ model with the new expanded domain and updated emissions as outlined in Sect. 3.3 were conducted for the period 10–21 January 2010, and compared with the forecast results. The model performance of the PM$_{10}$ in the model sensitivity testings are presented in this section.
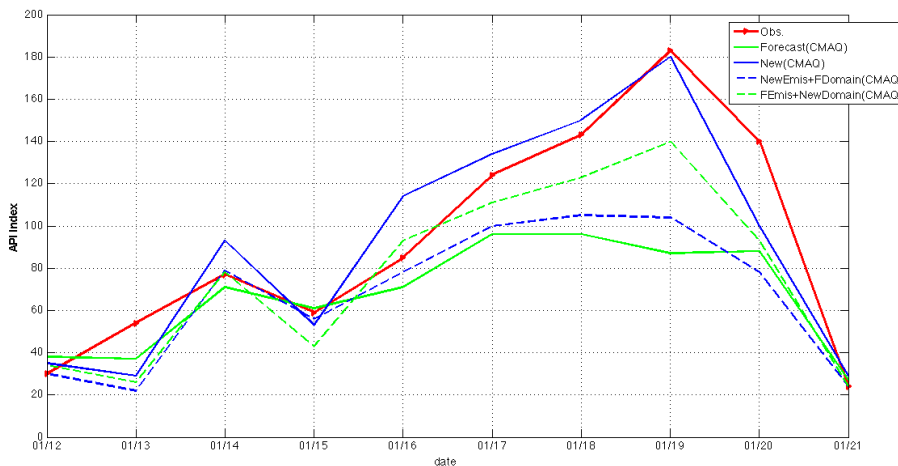
Figure 7. Comparison of measured and modelled daily averaged PM_{10}-API of the NSAQ stations in the Beijing urban area. After the improvement in model domain and emissions values, the "New(CMAQ)" results reach to the peak of the observations, which the forecast underestimated.
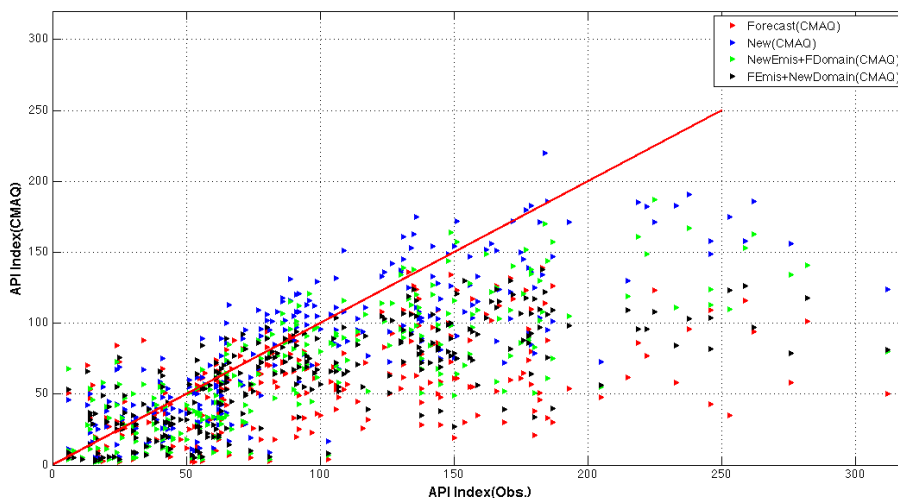

Figure 8. Scatter diagram of the observed and simulated PM_{10}-API of all stations in Beijing. Red indicates the original forecast results, and the blue triangles show the final model results, which are driven by the updated emissions in the expanded model domain, marked as "New(CMAQ)".

3.4.1 Model performance of the daily PM_{10}-API in the NSAQ stations

Figure 7 compares the measured and modelled daily averaged PM_{10}-API of the NSAQ stations in the Beijing urban area. The red and green solid line represents the observations and the forecast results in the forecast system. The model results driven by the updated emissions without expanding the model domain are abbreviated as "NewEmis+FDomain(CMAQ)" and are shown with the blue dashed line – the updated emissions include updated point and area source emissions. The modelled results driven by the forecast emissions in the expanded model domain are abbreviated as "FEmis+NewDomian(CMAQ)" and are shown

by the green dashed line. The blue solid line represents the final model results with all improvement methods and is named the "New(CMAQ)" in Fig. 7. These abbreviations are used with the same meanings in the following text.

Comparing the "Forecast(CMAQ)" and "FEmis+NewDomain(CMAQ)" results in Fig. 7, the averaged PM_{10}-API of the "FEmis+NewDomain(CMAQ)" results can reach 140, while the peak value of the PM_{10}-API in the forecast was about 100. The mean bias of the "FEmis+NewDomain(CMAQ)" is -15.4, better than the forecast -24.7. The normalized mean square error (NMSE) of the "FEmis+NewDomain(CMAQ)" is 0.082, also much better than the forecast 0.251, as shown in Table 2. The correlation coefficient increases from 0.895 to 0.943 when
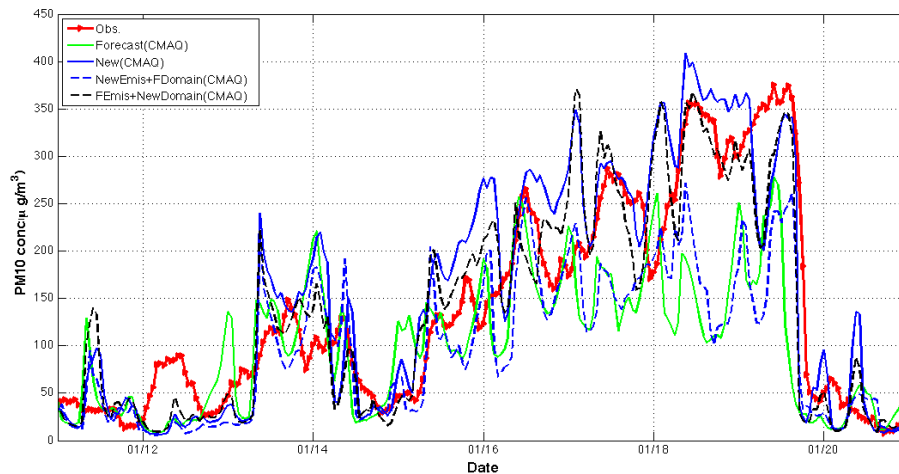
Figure 9. The time series of the PM_{10} hourly concentration during the air pollution episode in January 2010. The red solid line represents the observations, being the averaged PM_{10} hourly concentration observed in the 10 NSAQ stations in the Beijing MEMC monitoring network. The "New(CMAQ)" shows a much better model performance about the hourly concentration during the air pollution episode than the forecast due to the improvement of model domain and emissions.

the model domain is expanded with the forecast emissions in the CMAQ model. Furthermore, the air pollutant peak value of the "FEmis+NewDomain(CMAQ)" results occurs on 19 January, which is in agreement with the observations, while the forecast's peak appears on 18 January and shows little change between 17 and 20 January. This indicates that the expanded model domain can improve the simulation performance in capturing the air pollution peak. Thus, expanding the domain can improve the model performance clearly, even without the emissions being updated.

Comparing the forecast results and the model results when the emissions have been updated in the original forecast model domain, as shown by the "Forecast(CMAQ)" and "NewEmis+FDomain(CMAQ)" lines in Fig. 7, it is seen that the two lines are similar. The peak of the PM_{10}-API in the "NewEmis+FDomain(CMAQ)" is about 105, and the mean bias is -24.3, a little better than the forecast results. The NMSE between the "NewEmis+FDomain(CMAQ)" and the observations is 0.212, also slightly better than the forecast 0.251, as shown in Table 2. This indicates that the "NewEmis+FDomain" method showed a slight improvement in simulating the temporal variation of PM_{10} in the Beijing area.

However, in the "New" expanded model domain, the same updated emissions improve the model performance clearly. The "FEmis+NewDomain(CMAQ)" and "New(CMAQ)" shown in Fig. 7 are simulated in the same expanded model domain but are driven by the forecast emissions and the updated emissions, respectively. The peak of the "New(CMAQ)" reaches 180, much closer to the observed "red solid" line than the "FEmis+NewDomain(CMAQ)", the peak of which is about 140. And the mean bias of the "New(CMAQ)" is -0.2,

much better than the "FEmis+NewDomain(CMAQ)"; the NMSE of the "New(CMAQ)" is 0.042, also better than the 0.082 of the "FEmis+NewDomain(CMAQ)". The correlation coefficient of "New(CMAQ)" approaches that of the "FEmis+NewDomain(CMAQ)" at 0.931, shown in Table 2. This illustrates that the same updated emissions can improve the CMAQ model performance more clearly than the original forecast emissions in the expanded model domain.

From the two group comparisons of the updated emissions, it can be seen that the effect of updated emissions is clear in a suitable model domain, such as the expanded model domain in this paper. This may be attributed to more transport of pollutants in the surrounding areas are being included in the expanded domain. The CMAQ v4.4 model uses one-way nesting and only parts of variables are chosen as the boundary condition for the inner model domain, which will cause some underestimate through the boundary of the inner domain. The model sensitivity testings of another air quality model, CAMx, which uses two-way nesting, are presented in the Supplement. CAMx led to much better model performance when the emissions were updated without expanding the model domain –thus the two-way nested technology can help to reproduce the pollution transport process in this episode in the inner domain.

In the final model results with all improvement methods, the air pollutant peak value of the NSAQ station-averaged PM_{10}-API reaches 180 on 19 January, much closer to the observed "183" than the forecast "96". The mean bias of the "New(CMAQ)" to the observations is -0.2, much better than -24.7 in the forecast system, and the normal mean error (NME) is 15.9 %, also better than the 29.7 % in the forecast. The correlation coefficient of the averaged PM_{10}-API in NSAQ stations is 0.93, and higher than 0.89 between the

Table 2. Statistical measures of the modelled NSAQ station-averaged PM$_{10}$-API in Beijing.

	Obs.	Forecast	FEmis+ NewD omain(CMAQ)	NewEmis+FD omain(CMAQ)	New(CMAQ)
Peak	183	96	140	105	180
MB	–	−24.7	−15.4	−24.3	−0.2
NMSE	–	0.251	0.082	0.212	0.042
R	–	0.895	0.943	0.888	0.931

forecast and the observed. More significantly, the air pollutant peak value appears on 19 January, which is in agreement with the observations, illustrating that these methods improve the occurrence of the air pollutant peak simulated in the model.

3.4.2 Model performance of the daily PM$_{10}$-API in the all stations

We also collect the PM$_{10}$-API of all Beijing MEMC stations during the air pollution episode as mentioned in Sect. 3.2 and shown in the station map of Fig. 5 that covers all the Beijing counties.

A scatter diagram of the observed and simulated PM$_{10}$-API of all stations in the model sensitivity testings is shown in Fig. 8 – different colours stand for different model sensitivity testing results, and the statistical measures are presented in Table 3. The fraction of predictions within a factor of 2 of the observations (FAC2) and the normalized mean square error (NMSE) are selected to evaluate the model performance in this section. The FAC2 is the most robust measure, as it is not overly influenced by outliers (Chang and Hanna, 2004).

According to Fig. 8 and Table. 3, both the expanded model domain and the updated emissions can improve the model performance: the MB and NMSE decreases obviously, the FAC2 reaches 70 % and 68 %, and the correlation coefficient reaches 0.78 and 0.72, respectively. The "New(CMAQ)" results, which are driven by the updated emissions in the expanded model domain, include both aspects, and show the best performance.

As shown in the figure, the blue "New(CMAQ)" points have the highest simulated value, with the peak of the PM$_{10}$-API reaching 220, and the "New(CMAQ)" points are closer to the model perfect line "$y = x$" than the forecast's points. After the improvement, the mean bias of the "New(CMAQ)" is −15.7, much better than the forecast −43.2 in the PM$_{10}$-API simulation; the correlation coefficient of the PM$_{10}$-API in all stations between the "New(CMAQ)" and the observations is 0.82, obviously higher than the 0.54 between the forecast and the observed. And the FAC2 of the PM$_{10}$-API increases from 56 % in the forecast to 84 % in the final model results, which illustrates that there are more simulated samples that satisfy the FAC2 condition in the "New(CMAQ)" simulation. Furthermore, the NMSE of the PM$_{10}$-API is 0.196, which is also much better than the forecast's 0.886.

Based on the scatter plot (Fig. 8) and the statistical parameters MB, R, FAC2 and NMSE between the simulation and observation, we can see that the CMAQ model has a much better performance on the PM$_{10}$-API simulation in all Beijing MEMC stations in the "New(CMAQ)" than in the forecast due to the improvement of the model domain and emissions as discussed in Sect. 3.3.

3.4.3 Model performance of PM$_{10}$ hourly concentration

The observations of the PM$_{10}$ hourly concentration averages of NSAQ stations were provided by Beijing MEMC, and were used to evaluate the model's ability to simulate the hourly concentration.

As shown in Fig. 9, the forecast and model sensitivity testings show good model performance for hourly concentrations during the first and smaller air pollution episode process of 11–15 January, and records the occurrence of the smaller episode on 14 January. In the second and "bigger" air pollution episode process, the observed PM$_{10}$ concentration increases from 50 to 350 μg m^{-3} during the period 15–19 January. All the model sensitivity testings catch the first half of the accumulation process – the PM$_{10}$ hourly concentration increases from 50 to 250 μg m^{-3} from 15 to 16 January, and also shows good performance in the process when the hourly concentration rapidly decreases to "50 μg m^{-3} and lower" for several hours in the air pollutant dissipation process on 19 January.

But the forecast and "NewEmis+FDomain(CMAQ)" show no increases in the second half of the episode, where the observed hourly concentration increases from 250 to 350 μg m^{-3}, and the "FEmis+NewDomain(CMAQ)" and "New(CMAQ)" show better performance in PM$_{10}$ simulation, and the hourly concentration reaches 350 μg m^{-3}, which is the highest concentration in observed hourly concentration during the air pollution episode. Finally, the "New(CMAQ)" produces the best model performance, and the model sensitivity testings with the expanded domain show better model performance, no matter what the original forecast emissions.

That the performance of the "FEmis+NewDomian(CMAQ)" is better than "NewEmis+FDomain(CMAQ)" may be attributed to the regional transport of the pollutants being better reproduced with the expanded domain. This pollution episode was

Table 3. Statistical measures of the modelled daily PM_{10}-API of all stations in Beijing.

	Obs.	Forecast	FEmis+ New Domain(CMAQ)	NewEmis+F Domain(CMAQ)	New(CMAQ)
Peak	327	139	187	138	220
MB	–	−43.2	−30.4	−36.0	−15.7
NMSE	–	0.886	0.386	0.558	0.196
FAC2	–	56 %	70 %	68 %	84 %
R	–	0.54	0.78	0.72	0.82

reported by Zhao et al. (2013), who found that the pollutants in the Beijing area were significantly increased by regional transport from areas south of Beijing. In the forecast system, the pollutants outside of the inner domain (D4, covering Beijing) can only be transferred as a boundary condition to D4, and only a portion of the pollutants can by selected into boundary conditions. With the expanded domain, all the pollutants in the surrounding area can directly transport to Beijing, enhancing the results more than only increased emission without expanded domain.

Some statistical parameters of the PM_{10} hourly concentration in the forecast and "New(CMAQ)" are also presented in this study. The correlation coefficient between the simulation and observation increases from 0.77 in the forecast to 0.88 in the "New(CMAQ)", which indicates that the "New(CMAQ)" has a better tendency in hourly concentration. The FAC2 of the hourly concentration increases from 62 % in the forecast to 74 % in the "New(CMAQ)", and the NMSE decreases from 0.565 to 0.190 – both of which illustrate that the "New(CMAQ)" has better model performance than the forecast in the PM_{10} hourly concentration.

The forecast shows bad model performance in high concentration in the simulation, where the simulated hourly concentration is lower than $300\,\mu g\,m^{-3}$ in this air pollution episode, and the daily PM_{10}-API is lower than 150 during the entire duration of 2010, when the API is translated from the daily concentration. The improvement partly fixes this issue in that the PM_{10} hourly concentration in the "New(CMAQ)" can reach $350\,\mu g\,m^{-3}$, and the daily PM_{10}-API is able to reach 180 – both being closer to the observations.

4 Conclusions

The MM5-SMOKE-CMAQ model system has been used in EMS-Beijing for daily air quality forecast in recent years. In this study, we introduce the model set-up, meteorological field and emissions, including the emission inventory and processes in the forecast system. According to the model evaluation of PM_{10}-API for the entire duration of 2010, we found that the model shows a good model performance on most days but clearly underestimates some air pollution episodes. A typical air pollution episode was chosen to test

model improvement, including the set-up of model and emissions.

In summary, three numerical methods are adapted to the model improvement and presented in this study. First, we enhanced the inner "D4" domain, from 73×64 to 160×124 grids with 3 km grid resolution, to cover Beijing and its surrounding cities. Second, we added more regional point source emissions – 4405 point source emissions, located at Baoding, Landfang and Tangshan, were added into the point source emission inventory of the SMOKE model. Third, we increased the regional area source emissions in Baoding and Tangshan according to CCCPSC (2011), and updated Beijing area source emissions from the statistical county level to the village–town level to increase the resolution of the area emissions inventory.

Comparing the model evaluation of particle matter in different model sensitivity testings during the typical air pollution episode, we found that the hindcast ("New(CMAQ)"), including the expanded domain and updated emissions, shows a much better model performance. Obvious evidence of this is that the hindcast's averaged PM_{10}-API in NSAQ stations can reach 180, much closer to the observed "183", while its hourly concentration can reach the "observed" $350\,\mu g\,m^{-3}$, which the forecast cannot reach. In the simulation of the averaged PM_{10}-API of Beijing NSAQ stations, the mean bias of the hindcast decreases to −0.2, the normal mean error to 15.9 %, and the correlation coefficient increases to 0.93. For PM_{10}-API of all stations in Beijing, the FAC2 increases from 56 % in the forecast to 84 % in the hindcast, while the NMSE decreases from 0.886 to 0.196. In the simulation of the PM_{10} hourly concentration, the correlation coefficient increases from 0.77 in the forecast to 0.88 in the hindcast, the FAC2 increases from 62 % to 74 %, and the NMSE decreases from 0.565 to 0.190. All of this illustrates the hindcast gives a much better model performance than the forecast in PM_{10} simulation of Beijing stations, not only for the daily concentration but also for the hourly concentration.

The improvement methods we have applied in this study will be helpful to enhance the model performance in forecasting the air quality in Beijing and surrounding area. In particular, expanding the model domain indicated that a suitable domain setting is very important for the regional transport process, which is a key point in air quality forecasting not

only in Beijing but also for other similar regions. The modified emission inventory can also be used in future forecasting and modelling works.

In the future, more model evaluation and improvement will continue in the air quality forecast in Beijing, to find other underestimated or overestimated cases in yearly forecasts and discover their causes, in order to improve the air quality forecast in those megacities, not only in Beijing.

Table A1. API values and corresponding pollutant concentration (daily, unit: mg m^{-3}).

API	SO$_2$	NO$_2$	PM$_{10}$
50	0.05	0.08	0.05
100	0.15	0.12	0.15
200	0.80	0.28	0.35
300	1.60	0.565	0.42
400	2.10	0.75	0.50
500	2.62	0.94	0.60

Appendix A: The air pollution index of particulate matter calculation

The model's SO$_2$-API, NO$_2$-API and PM$_{10}$-API were calculated as follows, as defined by China EPB:

$$\text{API} = \frac{I_{\max} - I_{\min}}{C_{\max} - C_{\min}} \times (C - C_{\min}) + I_{\min},$$

where C is concentration of the pollutant, $C_{\max}/C_{\min}$ is the classic concentration shown in Table A1 near to C, and the $I_{\max}/I_{\min}$ are the corresponding API values.

Taking the PM$_{10}$-API value for example, if the observation of PM$_{10}$ concentration is 0.12 mg m^{-3}, then, $C = 0.12$ mg m^{-3}, and $C_{\max}$ and $C_{\min}$ are 0.050 mg m^{-3} and 0.150 mg m^{-3}, respectively, and $I_{\max}$ and $I_{\min}$ are 50 and 100. Thus, the API of PM$_{10}$ concentration (0.12 mg m^{-3}) is calculated as

$$\text{API} = \frac{100 - 50}{0.150 - 0.050} \times (0.12 - 0.050) + 50 = 85.$$

Appendix B: The statistical parameters

Mean bias:

$$\text{MB} = \frac{1}{n} \sum_{i=1}^{n} (\text{Sim}(i) - \text{Obs}(i)).$$

Normal mean error:

$$\text{NME} = \frac{1}{n} \sum_{i=1}^{n} |\text{Sim}(i) - \text{Obs}(i)| / \text{Obs}(i).$$

Correlation coefficient (R):

$$R = \frac{\sum_{i=1}^{n} (\text{Sim}(i) - \overline{\text{Sim}})(\text{Obs}(i) - \overline{\text{Obs}})}{\sqrt{\sum_{i=1}^{n} (\text{Sim}(i) - \overline{\text{Sim}})^2 \sum_{i=1}^{n} (\text{Obs}(i) - \overline{\text{Obs}})^2}}.$$

The normalized mean square error (NMSE):

$$\text{NMSE} = \frac{\overline{(\text{Obs} - \text{Sim})^2}}{\overline{\text{Obs}} \times \overline{\text{Sim}}}.$$

FAC2 (fraction of predictions within a factor of 2 of the observations) = fraction of data that satisfies

$$0.5 \leq \frac{\text{Sim}(i)}{\text{Obs}(i)} \leq 2.0.$$

Code availability

We use the original code CMAQ v4.4 as distributed by Community Modeling & Analysis System (CMAS, https://www.cmascenter.org/). The model source code and the configuration, the library files and build scripts are all in the zipped file, which is accessible via ftp://159.226.119.102:/CMAQ2GMD.zip. The model runs on CentOS 5.5 Linux with PGI Fortran Compiler.

The Supplement related to this article is available online at doi:10.5194/gmd-7-2243-2014-supplement.

References

An, X., Zhu, T., Wang, Z., Li, C., and Wang, Y.: A modeling analysis of a heavy air pollution episode occurred in Beijing, Atmos. Chem. Phys., 7, 3103–3114, doi:10.5194/acp-7-3103-2007, 2007.

Appel, K. W., Roselle, S. J., Gilliam, R. C., and Pleim, J. E.: Sensitivity of the Community Multiscale Air Quality (CMAQ) model v4.7 results for the eastern United States to MM5 and WRF meteorological drivers, Geosci. Model Dev., 3, 169–188, doi:10.5194/gmd-3-169-2010, 2010.

Beijing EPB: State of the Environment Bulletin in the year 2010, available at: http://www.bjepb.gov.cn/bjepb/341240/index.html (last access: June 2011), 2011.

Binkowski, F. S. and Roselle, S. J.: Models-3 Community Multiscale Air Quality (CMAQ) model aerosol component 1. Model description, J. Geophys. Res.-Atmos., 108, 4183, doi:10.1029/2001JD001409, 2003.

Briggs, G.: Discussions on chimney plumes in neutral and stable surroundings, Atmos. Environ., 6, 507–510, 1972.

Briggs, G. A.: Plume rise and buoyancy effects, in: Atmospheric Science and Power Production, 327–366, 1984.

BTRC: Beijing Transport Annual Report 2006, Tech. rep., Beijing Transport Research Center, Beijing, China, 2007.

Byun, D. and Ching, J. K. S.: Science Algorithms of the EPA Models-3 Community Multi-scale Air Quality (CMAQ) Modeling System, Tech. Rep. EPA/600/R-99/030, US EPA National Exposure Research Laboratory, Research Triangle Park, NC, 1999.

Byun, D. and Schere, K. L.: Review of the governing equations, computational algorithms, and other components of the Models-3 Community Multiscale Air Quality (CMAQ) modeling system, Appl. Mech. Rev., 59, 51–77, 2006.

Cao, G., Zhang, X., Gong, S., An, X., and Wang, Y.: Emission inventories of primary particles and pollutant gases for China, Chinese Sci. Bull., 56, 781–788, 2011.

CCCPSC: The Pollution Source Census Data Set (Statistic), Collected Works about the First China Pollution Source Survey Data (V), Compilation Committee of China Pollution Source Census I, China Environment Science Press, Beijing, 228–245, 2011.

Chang, J. and Hanna, S.: Air quality model performance evaluation, Meteorol. Atmos. Phys., 87, 167–196, 2004.

Cruickshank, T. S.: CMAQ sensitivity to winter-time ground surface albedo, in: Proceedings of the 7th Annual Community Modeling and Analysis (CMAS) Conference: Model Evaluation and Analysis, Chapel Hill, NC, 2008.

Demerjian, K. L., Schere, K. L., and Peterson, J. T.: Theoretical Estimates of Actinic (Spherically Integrated) Flux and Photolytic Rate Constants of Atmospheric Species in the Lower Troposphere, John Wiley & Sons, New York, NY, 369–459, 1980.

Dobson, J. E., Bright, E. A., Coleman, P. R., Durfee, R. C., and Worley, B. A.: LandScan: a global population database for estimating populations at risk, Photogramm. Eng. Remote. S., 66, 849–857, 2000.

ENVIRON: User's Guide to the Comprehensive Air Quality Modeling System with Extensions (CAMx), Version 4.4, Tech. Rep. 10, p. 16, p. 29, 38–40, p. 30, p. 44, ENVIRON, 2002.

Feng, Y., Wang, A., Wu, D., and Xu, X.: The influence of tropical cyclone Melor on PM_{10} concentrations during an aerosol episode over the Pearl River Delta region of China: numerical modeling versus observational analysis, Atmos. Environ., 41, 4349–4365, 2007.

Gao, Y., He, J., and Wang, Z.: Simulation for impact of urbanization on meteorological conditions in Beijing area, J. Meteorol. Environ., 23, 58–64, 2007 (in Chinese).

Gery, M. W., Whitten, G. Z., Killus, J. P., and Dodge, M. C.: A photochemical kinetics mechanism for urban and regional scale computer modeling, J. Geophys. Res.-Atmos., 94, 12925–12956, 1989.

Grell, G. A., Dudhia, J., and Stauffer, D. R.: A description of the Fifth-Generation Penn State/NCAR Mesoscale Model (MM5), Tech. Rep. NCAR/TN-398+STR, Natl. Cent. for Atmos. Res., Boulder, Colo., 1994.

Hao, J., Wang, L., Shen, M., Li, L., and Hu, J.: Air quality impact of power plant emissions in Beijing, Environ. Pollut., 147, 401–408, 2008.

Houyoux, M. R. and Vukovich, J. M.: Updates to the Sparse Matrix Operator Kernel Emissions (SMOKE) modeling system and integration with Models-3, The Emission Inventory: Regional Strategies for the Future, Air Waste Management Association, Raleigh, N.C., 1461, 1999.

Mobley, J. D., Beck, L. L., Sarwar, G., Reff, A., and Houyoux, M.: SPECIATE – EPA's Database of Speciated Emission Profiles, in: 6th Annual CMAS Conference, US Environmental Protection Agency, Chapel Hill, NC, 2007.

Streets, D., Bond, T., Carmichael, G., Fernandes, S. D., Q. Fu, D. H., Klimont, Z., Nelson, S. M., Tsai, N. Y., Wang, M. Q., Woo, J. H., and Yarber, K. F.: An inventory of gaseous and primary aerosol emission in Asia in the year 2000, J. Geophys. Res.-Atmos., 108, 8809, doi:10.1029/2002JD003093, 2003.

Streets, D., Zhang, Q., Wang, L., He, K., Hao, J., Wu, Y., Tang, Y., and Carmichael, G. R.: Revisiting China's CO emissions af-

ter the Transport and Chemical Evolution over the Pacific (TRACE-P) mission: synthesis of inventories, atmospheric modeling, and observations, J. Geophys. Res.-Atmos., 111, D14306, doi:10.1029/2006JD007118, 2006.

Streets, D., Joshua, S. F., Carey, J., Hao, J., He, K., Tang, X., Zhang, Y., Wang, Z., Li, Z., Zhang, Q., Wang, L., Wang, B., and Yu, C.: Air quality during the 2008 Beijing Olympic Games, Atmos. Environ., 41, 480–492, 2007.

UNC: SMOKE v2.7 User's Manual, Tech. Rep. 98, The institute for the Environment – The University of North Carolina at Chapel Hill, 2010.

Wang, S., Zhao, M., Xing, J., Wu, Y., Zhou, Y., Lei, Y., He, K., Fu, L., and Hao, J.: Quantifying the air pollutants emission reduction during the 2008 Olympic Games in Beijing, Environ. Sci. Technol., 44, 2490–2496, 2010.

Wang, Z., Xie, F., Wang, X., An, J., and Zhu, J.: Development and application of nested air quality prediction modeling system, Chinese J. Atmos. Sci., 30, 778–790, 2006 (in Chinese).

Wang, Z., Wu, Q., Gbaguidi, A., Yan, P., Zhang, W., Wang, W., and Tang, X.: Ensemble air quality multi-model forecast system for Beijing (EMS-Beijing): model description and preliminary application, J. Nanjing University Inform. Sci. Technol.: Natural Science Edition, 1, 19–26, 2009 (in Chinese).

Wu, Q.: Air Quality Multi-models real-time forecast system in Beijing and its Air Quality Multi-models real-time forecast system in Beijing and its application, Ph.D. thesis, Institute of Atmospheric Physics, Chinese Academy of Sciences, Beijing, 2010a.

Wu, Q., Wang, Z., Xu, W., Huang, J., and Gbaguidi, A.: Multi-model simulation of PM$_{10}$ during the 2008 Beijing Olympic Games: effectiveness of emission restrictions, Acta Scientiae Circumstantiae, 30, 1739–1748, 2010a (in Chinese).

Wu, Q., Wang, Z., and Cui, Y.: Evaluating the solar radiation resources of China recent 20 years by meteorologieal model, J. Appl. Meteorol. Sci., 21, 343–351, 2010b (in Chinese).

Wu, Q., Wang, Z., Alex, G., Tang, X., and Zhou, W.: Numerical study of the effect of traffic restriction on air quality in Beijing, SOLA, 6A, 017–020, 2010c.

Wu, Q., Wang, Z. F., Gbaguidi, A., Gao, C., Li, L. N., and Wang, W.: A numerical study of contributions to air pollution in Beijing during CAREBeijing-2006, Atmos. Chem. Phys., 11, 5997–6011, doi:10.5194/acp-11-5997-2011, 2011.

Wu, Q., Wang, Z., Chen, H., Zhou, W., and Wenig, M.: An evaluation of air quality modeling over the Pearl River Delta during November 2006, Meteorol. Atmos. Phys., 116, 113–132, doi:10.1007/s00703-011-0179-z, 2012.

Zhang, M., Uno, I., Zhang, R., Han, Z., Wang, Z., and Pu, Y.: Evaluation of the Models-3 Community Multi-scale Air Quality (CMAQ) modeling system with observations obtained during the TRACE-P experiment: comparison of ozone and its related species, Atmos. Environ., 40, 4874–4882, 2006.

Zhang, Q., Streets, D. G., Carmichael, G. R., He, K. B., Huo, H., Kannari, A., Klimont, Z., Park, I. S., Reddy, S., Fu, J. S., Chen, D., Duan, L., Lei, Y., Wang, L. T., and Yao, Z. L.: Asian emissions in 2006 for the NASA INTEX-B mission, Atmos. Chem. Phys., 9, 5131–5153, doi:10.5194/acp-9-5131-2009, 2009.

Zhao, B., Wang, P., Ma, J. Z., Zhu, S., Pozzer, A., and Li, W.: A high-resolution emission inventory of primary pollutants for the Huabei region, China, Atmos. Chem. Phys., 12, 481–501, doi:10.5194/acp-12-481-2012, 2012.

Zhao, X. J., Zhao, P. S., Xu, J., Meng,, W., Pu, W. W., Dong, F., He, D., and Shi, Q. F.: Analysis of a winter regional haze event and its formation mechanism in the North China Plain, Atmos. Chem. Phys., 13, 5685-5696, doi:10.5194/acp-13-5685-2013, 2013.